

Peculiar Velocities of Galaxy Clusters

J.M. Colberg,¹ S.D.M. White,¹ T.J. MacFarland,^{2,3} A. Jenkins,⁴
 F.R. Pearce,⁴ C.S. Frenk,⁴ P.A. Thomas,⁵ H.M.P. Couchman⁶

¹*Max-Planck-Institut für Astrophysik, Karl-Schwarzschild-Str. 1, D-85740 Garching, Germany*

²*Rechenzentrum Garching, Boltzmannstr. 2, D-85740 Garching, Germany*

³*now at Enterprise Architecture Group, Global Securities Industry Group, 1185 Avenue of the Americas, New York 10036, USA*

⁴*Physics Dept., University of Durham, Durham DH1 3LE, UK*

⁵*CEPS, University of Sussex, Brighton BN1 9QH, UK*

⁶*Dept. of Astronomy, University of Western Ontario, London, Ontario N6A 3K7, Canada*

4 April 2021

ABSTRACT

We investigate the peculiar velocities predicted for galaxy clusters by theories in the cold dark matter family. A widely used hypothesis identifies rich clusters with high peaks of a suitably smoothed version of the linear density fluctuation field. Their peculiar velocities are then obtained by extrapolating the similarly smoothed linear peculiar velocities at the positions of these peaks. We test these ideas using large high resolution N-body simulations carried out within the Virgo supercomputing consortium. We find that at early times the barycentre of the material which ends up in a rich cluster is generally very close to a high peak of the initial density field. Furthermore the mean peculiar velocity of this material agrees well with the linear value at the peak. The late-time growth of peculiar velocities is, however, systematically underestimated by linear theory. At the time clusters are identified we find their *rms* peculiar velocity to be about 40% larger than predicted. Nonlinear effects are particularly important in superclusters. These systematics must be borne in mind when using cluster peculiar velocities to estimate the parameter combination $\sigma_8\Omega^{0.6}$.

Key words: cosmology: theory – large-scale structure of Universe, cosmology: theory – dark matter, galaxies: clusters

1 INTRODUCTION

The motions of galaxy clusters are thought to result from gravitational forces acting over the very large scales on which superclusters are assembled. The *rms* deviations from uniformity on such scales appear to be small, and so may be adequately described by the linear theory of fluctuation growth. For a linear density field of given power spectrum the *rms* peculiar velocity is proportional to $\sigma_8\Omega^{0.6}$ where Ω is the cosmic density parameter and σ_8 , the *rms* mass fluctuation in a sphere of radius $8 h^{-1}\text{Mpc}$, is a conventional measure of the amplitude of fluctuations (e.g. Peebles 1993). (As usual the Hubble constant is expressed as $H_0 = 100 h \text{ km/sec/Mpc}$.) Distance indicators such as the Tully-Fisher or D_n - σ relations allow the peculiar velocities of clusters to be measured, thus providing a direct estimate of this parameter combination (see, for example, Strauss & Willick 1996).

Essentially the same parameter combination can also be estimated from the *abundance* of galaxy clusters (e.g. White et al. 1993) and a comparison of the two estimates could in principle provide a check on the shape of the assumed power spectrum and on the assumption that the initial density field

had gaussian statistics. In practice this is difficult because of the uncertainties in relating observed cluster samples to the objects for which quantities are calculated in linear theory or measured from N-body simulations. The standard linear model was introduced by Bardeen et al. (1986; hereafter BBKS). It assumes that clusters can be identified with “sufficiently” high peaks of the linear density field after convolution with a “suitable” smoothing kernel. The peculiar velocity of a cluster is identified with the linear peculiar velocity of the corresponding peak extrapolated to the present day. In the present paper we study the limitations both of this model and of direct N-body simulations by comparing their predictions for clusters on a case by case basis.

In the next section we summarize both the linear predictions for the growth of peculiar velocities and the BBKS formulae for the values expected at peaks of the smoothed density field. Section 3 then presents our set of N-body simulations and outlines our procedures for identifying peaks in the initial conditions and clusters at $z = 0$. Section 4 begins by studying how well peaks correspond to the initial barycentres of clusters; we then show that the smoothed

linear velocity at a peak agrees well with the mean linear velocity of its cluster; finally we show that the growth of cluster peculiar velocities is systematically stronger at late times than linear theory predicts. A final section presents a brief discussion of these results.

2 LINEAR PREDICTIONS FOR THE PECULIAR VELOCITIES OF PEAKS

2.1 The Growth of Peculiar Velocities

According to the linear theory of gravitational instability in a dust universe (Peebles 1993), the peculiar velocity of every mass element grows with cosmic scale factor a as

$$v \propto a\dot{D}, \quad (1)$$

where $a(t)$ is obtained from the Friedman equation

$$\left(\frac{\dot{a}}{a}\right)^2 = \Omega_0 a^{-3} + (1 - \Omega_0 - \Lambda_0) a^{-2} + \Lambda_0, \quad (2)$$

and $D(t)$ is the growth factor for linear density perturbations, $\delta(\mathbf{x}, t) = D(t)\delta_0(\mathbf{x})$. Ω_0 and Λ_0 are the density parameter and the cosmological constant at $z = 0$, respectively, and we define $a = 1$ at this time. A number of accurate approximate forms are known for the relations between D and a and can be used to cast the scaling of eq. (1) into a more convenient form. We write

$$\dot{D} \equiv \frac{dD}{dt} = \frac{dD}{da} \frac{da}{dt}, \quad (3)$$

and substitute for da/dt from the Friedman equation (2). Lahav et al. (1991) give an approximation for dD/da in the combination

$$f(a) \equiv \frac{dD}{da} \frac{a}{D} \approx \left(\frac{\Omega_0 a^{-3}}{\Omega_0 a^{-3} + (1 - \Omega_0 - \Lambda_0) a^{-2} + \Lambda_0} \right)^{0.6}. \quad (4)$$

For $a = 1$ this gives the standard factor $f \approx \Omega_0^{0.6}$ which appears when predicting the peculiar velocities produced by a given overdensity field. Carroll et al. (1992) used this result to derive an approximation for $D(a)$ itself,

$$D \approx a g(a), \quad (5)$$

where

$$g(a) = \frac{5}{2} \frac{\Omega_0(a)}{\Omega^{4/7}(a) - \Lambda(a) + \left(1 + \frac{\Omega(a)}{2}\right) \left(1 + \frac{\Lambda(a)}{70}\right)} \quad (6)$$

with

$$\Omega(a) = \frac{\Omega_0}{a + \Omega_0(1 - a) + \Lambda(a^3 - a)}, \quad (7)$$

$$\Lambda(a) = \frac{\Lambda a^3}{a + \Omega_0(1 - a) + \Lambda(a^3 - a)}. \quad (8)$$

Combining these equations, we obtain an explicit approximation for the growth of peculiar velocities,

$$v \propto f(a) g(a) a^2 \sqrt{\Omega_0 a^{-3} + (1 - \Omega_0 - \Lambda_0) a^{-2} + \Lambda_0}. \quad (9)$$

For the simple Einstein-de Sitter case where $\Omega_0 = 1$ and $\Lambda = 0$, these formulae reduce to the exact results $D = a \propto t^{2/3}$ and $v \propto \sqrt{a}$.

Recently, Eisenstein (1997) has shown that the exact solutions for D and $f(a)$ can be given explicitly in terms of

elliptic integrals. He also shows that the above approximations always have fractional errors better than 2% if $\Omega > 0.1$. We therefore work with the simpler approximate formulae in the present paper.

2.2 The Velocities of Peaks

The idea that the statistical properties of nonlinear objects like galaxy clusters can be inferred from the initial linear density field was developed in considerable detail in the monumental paper of Bardeen et al. (1986; BBKS). If the initial fluctuations are assumed to be a gaussian random field, they are specified completely by their power spectrum, $P(k)$. Similarly, any smoothed version of this initial field is specified completely by its own power spectrum, $P(k)W^2(kR)$, where $W(kR)$ is the Fourier transform of the spherical smoothing kernel and R is a measure of its characteristic radius. In particular, BBKS showed how the abundance and *rms* peculiar velocity of peaks of given height can be expressed in terms of integrals over $P(k)W^2(kR)$. The difficulty in connecting this model with real clusters lies in the ambiguity in deciding what smoothing kernel, characteristic scale, and peak height are appropriate. Typically the smoothing kernel is taken to be a gaussian or a top-hat, R is chosen so that the kernel contains a mass similar to the minimum mass of the cluster sample, and the height is assumed sufficient for a spherical perturbation to collapse by $z = 0$.

The smoothed initial peculiar velocity field is isotropic and gaussian with a three-dimensional dispersion given by

$$\sigma_v(R) \equiv H \Omega^{0.6} \sigma_{-1}(R), \quad (10)$$

where, in the notation of BBKS, σ_j is defined for any integer j by

$$\sigma_j^2(R) = \frac{1}{2\pi^2} \int P(k) W^2(kR) k^{2j+2} dk. \quad (11)$$

The *rms* peculiar velocity at peaks of the smoothed density field differs systematically from σ_v ; BBKS show that it is given by

$$\sigma_p(R) = \sigma_v(R) \sqrt{1 - \sigma_0^4 / \sigma_1^2 \sigma_{-1}^2}. \quad (12)$$

Note that this expression does not depend on the height of the peaks. As shown in BBKS, the velocities of peaks are *statistically* independent of their height.

Throughout this paper we will approximate the power spectra of CDM models by the parametric expression of Bond & Efstathiou (1984),

$$P(k, \Gamma) = \frac{Ak}{\{1 + [ak/\Gamma + (bk/\Gamma)^{3/2} + (ck/\Gamma)^2]^\nu\}^{2/\nu}}, \quad (13)$$

where $a = (6.4/\Gamma) h^{-1}$ Mpc, $b = (3.0/\Gamma) h^{-1}$ Mpc, $c = (1.7/\Gamma) h^{-1}$ Mpc, $\nu = 1.13$, and the shape parameter Γ is given for the models discussed below by

$$\Gamma = \begin{cases} \Omega_0 h / [0.861 + 3.8(m_{10}^2 \tau_d)^{2/3}]^{1/2} & \text{for } \tau\text{CDM,} \\ \Omega_0 h & \text{otherwise.} \end{cases} \quad (14)$$

In the τ CDM case m_{10} is the τ -neutrino mass in units of 10 keV and τ_d is its lifetime in years (White et al. 1995). A detailed investigation of this model can be found in Bharadwaj & Sethi (1998). For the cosmologies used here, we take the values shown in Table 1. Detailed calculations of the

power spectrum are actually better fit by slightly smaller values of Γ than we assume (Sugiyama 1995).

The normalisation constant in equation (13) can be related to the conventional normalisation σ_8 by noting that $\sigma_8 \equiv \sigma_0(8h^{-1}\text{Mpc})$ and using equation (11) with a top-hat window function, $W_{TH}(x) = 3(x \sin x - \cos x)/x^3$. This corresponds to the linear fluctuation amplitude extrapolated to $z = 0$ and can be matched to observation by fitting either to the cosmic microwave background fluctuations measured by COBE or to the observed abundance of rich galaxy clusters. The models of this paper are normalised using the second method (c.f. Eke et al. 1996), as reflected by the σ_8 values given in Table 1 together with the other parameters defining the models.

In the following linear density fields are smoothed either with a top-hat or with a gaussian. In the latter case the window function is $W_G(x) = \exp[-x^2/2]$. It is unclear for either filter how R should be chosen in order to optimize the correspondance between peaks and clusters. We follow previous practice in assuming that cluster samples contain all objects with mass exceeding some threshold M_{min} , and then choosing R so that the filter contains M_{min} . Hence $M_{min} = 4\pi\bar{\rho}R^3/3$ in the top-hat case and $M_{min} = (2\pi)^{3/2}\bar{\rho}R^3$ in the gaussian case. The simulations analysed here have $\Omega_0 = 0.3$ or 1.0 , and we will isolate cluster samples limited at $M_{min} = 3.5 \times 10^{14}h^{-1}M_\odot$, the value appropriate for Abell clusters of richness one and greater (e.g. White et al. 1993). A detailed discussion of filtering schemes can be found in Monaco (1998) and references therein.

Table 2 gives characteristic filter radii R and values of σ_v and σ_p from equations (11) and (13) for both smoothings and for all the cosmological models we consider in this paper; the velocity dispersions are extrapolated to the linear values predicted at $z = 0$. The difference between σ_v and σ_p has often been ignored in the literature when predicting the peculiar velocities of galaxy clusters (e.g. Croft & Efstathiou 1994; Bahcall & Oh 1996; Borgani et al. 1997); for our models the two differ by about 15%. Notice also that with our choice of filter radii, gaussian smoothing predicts *rms* peculiar velocities about 10% smaller than top-hat smoothing.

3 THE SIMULATIONS

3.1 The Code

The Virgo Consortium was formed in order to study the evolution of structure and the formation of galaxies using the latest generation of parallel supercomputers (Jenkins et al. 1996). The code used for the simulations of this paper is called HYDRA. The original serial code was developed by Couchman et al. (1995) and was parallelized for CRAY T3D's by Pearce et al. (1995) (A detailed description can be found in Pearce & Couchman (1997). T3D-HYDRA is a parallel adaptive particle-particle/particle-mesh (AP³M) code implemented in CRAFT, a directive-based parallel Fortran developed by CRAY. It supplements the standard P³M algorithm (Efstathiou et al. 1985) by recursively placing higher resolution meshes, *refinements*, over heavily clustered regions. Refinements containing more than $\sim 10^5$ particles are executed in parallel by all processors; smaller refinements

Table 1. The Virgo models

Model	Ω	Λ	h	σ_8	Γ	z_{Start}
OCDM	0.3	0.0	0.7	0.85	0.21	119
Λ CDM	0.3	0.7	0.7	0.90	0.21	30
SCDM	1.0	0.0	0.5	0.51	0.50	35
τ CDM	1.0	0.0	0.5	0.51	0.21	35

are completed using a task farm approach. This T3D version currently includes an SPH treatment of gas dynamics, but this was not used for the simulations of this paper.

A second version of HYDRA, based on CRAY's shared memory and message passing architecture, has been written by MacFarland et al. (1997). This can run on CRAY T3E's but does not currently include refinement placing.

The simulations used here were run on the Cray T3D and T3E supercomputers at the computer center of the Max Planck Society in Garching and at the Edinburgh Parallel Computing Centre.

3.2 The Simulation Set

A set of four matched N-body simulations of CDM universes was completed in early 1997. Each follows the evolution of structure within a cubic region $240h^{-1}\text{Mpc}$ on a side using 256^3 equal mass particles and a gravitational softening of $30h^{-1}\text{kpc}$. The choices of cosmological parameters correspond to standard CDM (SCDM), to an Einstein-de Sitter model with an additional relativistic component (τ CDM), to an open CDM model (OCDM), and to a flat low density model with a cosmological constant (Λ CDM). A list of the parameters defining these models is given in Table 1.

In all models the initial fluctuation amplitude, and so the value of σ_8 , was set by requiring that the models should reproduce the observed abundance of rich clusters. Further details of this choice and of other aspects of the simulations can be found in Jenkins et al. (1998). Note that each Fourier component of the initial fluctuation field had the same *phase* in each of these four simulations. As a result there is an almost perfect correspondance between the clusters in the four models.

Because of their finite volume, these simulations contain no power at wavelengths longer than $240h^{-1}\text{Mpc}$. Furthermore, Fourier space is sampled quite coarsely on the largest scales for which they do contain power, and so realisation to realisation fluctuations on these scales can be significant. The size of the effects can be judged from Table 2 where we list the values of σ_v and σ_p obtained for each model when the theoretical power spectrum is replaced in equations (11) and (13) by the initial power spectrum of the model itself. These are systematically smaller than the values found before. The difference is primarily a reflection of the loss of large-scale power.

3.3 The Selection of Peaks

We identify peaks in the initial conditions of the simulations by binning up the initial particle distribution on a 128^3 mesh using a cloud-in-cell (CIC) assignment and then smoothing with a gaussian or a top-hat with characteristic scale R corresponding to $M_{min} = 3.5 \times 10^{14}h^{-1}M_\odot$. A peak

Table 2. For each of the models, the following quantities are given: the radius R (second and fifth column) of the filter used in eq. (12); the three-dimensional velocity dispersions σ_v and σ_p (third, fourth, sixth, and seventh column) obtained using eq.s (11) and (13) with the given filter radii; the three-dimensional velocity dispersions σ_v and σ_p (eighth, ninth, eleventh, and twelfth column) obtained using eq.s (11) and (13) with the given filter radii and the power spectra of the simulations themselves; the *rms* linear overdensity Δ (tenth and thirteenth column) smoothed with the given filter radii and extrapolated to $z = 0$; the number of clusters N_{Cl} (fourteenth column) found in the simulations at $z = 0$; the three-dimensional velocity dispersions of peaks (fifteenth and sixteenth column) in the initial conditions of the simulations using the given filters; the three-dimensional linear velocity dispersions of clusters extrapolated to $z = 0$; and the three-dimensional measured velocity dispersion of clusters at $z = 0$. The radii are given in Mpc/h , the velocity dispersions in km/sec . Top Hat and Gaussian filters are abbreviated as TH and G, respectively.

(1) Model	Top-Hat			Gaussian			Sim TH			Sim Gauss			TH	G	Sim	Sim	
	(2) R	(3) σ_v	(4) σ_p	(5) R	(6) σ_v	(7) σ_p	(8) σ_v	(9) σ_p	(10) Δ	(11) σ_v	(12) σ_p	(13) Δ	(14) N_{Cl}	(15) σ_{Peak}	(16) σ_{Peak}	(17) σ_{in}	(18) $\sigma_{z=0}$
OCDM	10.3	390	349	6.6	366	315	351	300	0.94	321	258	0.96	62	253	266	280	407
Λ CDM	10.3	413	370	6.6	387	334	371	318	0.98	340	272	1.03	69	296	323	300	439
SCDM	6.9	381	334	4.4	349	290	375	325	0.58	342	278	0.60	92	308	318	307	425
τ CDM	6.9	509	464	4.4	485	430	464	412	0.57	437	371	0.58	70	392	399	398	535

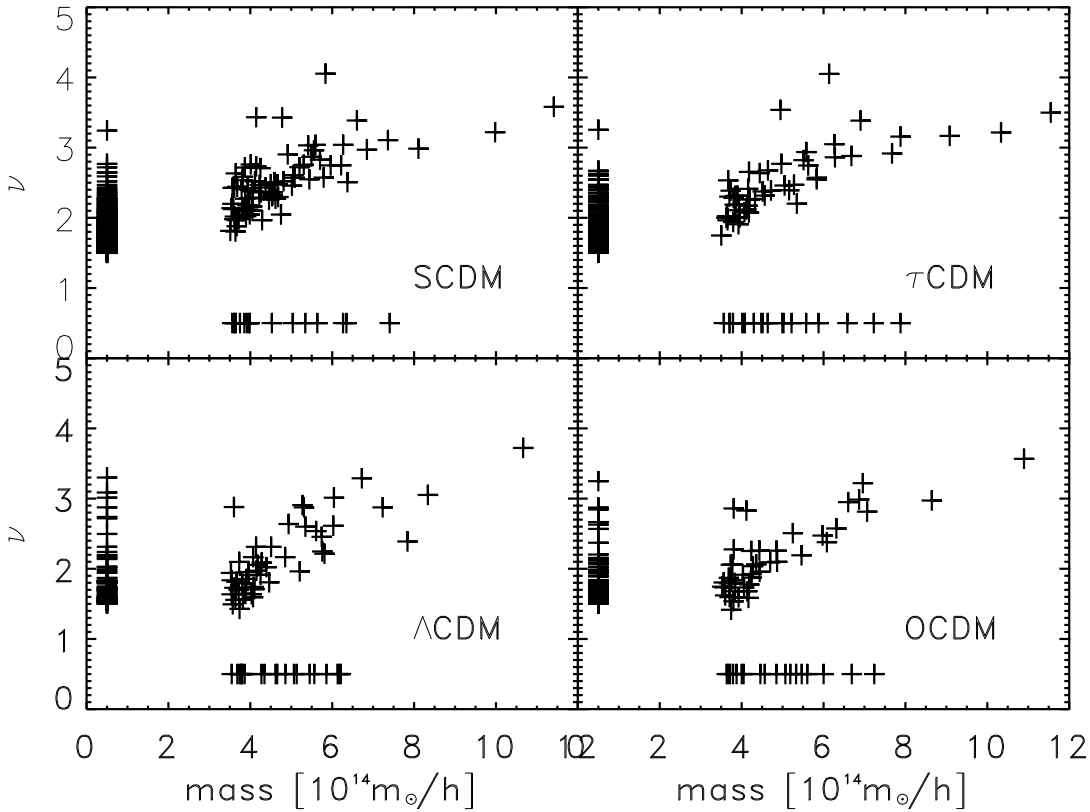


Figure 1. The mass of the clusters in our simulations against the height of the corresponding peaks in the initial conditions, once these are smoothed with a top-hat with the characteristic radius listed in Table 2. All clusters with mass greater than $3.5 \times 10^{14} h^{-1} M_{\odot}$ and all peaks with height greater than $\nu = 1.5$ are shown. There are 351, 239, 84, and 83 unmatched peaks in the SCDM, τ CDM, Λ CDM, and OCDM model, respectively.

is then taken to be any grid point at which the smoothed density is greater than that of its 26 nearest neighbours. The dimensionless height of a peak, ν , is defined by dividing its overdensity by the *rms* overdensity, Δ , which we list in Table 2. Again, within the matched set there is a close correspondance between the peaks found in the four models. In addition, the peaks found with gaussian smoothing correspond closely to those found with top-hat smoothing.

Particle peculiar velocities are binned up and smoothed in an identical way and the peculiar velocity of a peak is

taken to be the value at the corresponding grid point. In Table 2 we list the *rms* peculiar velocity of the peaks found in each model. Again this is scaled up to the value expected at $z = 0$ according to linear theory. It differs slightly from the value predicted by inserting the power spectrum of the simulation directly into equation (13) because there are realisation to realisation fluctuations depending on the *phases* of the Fourier components. As it should, the *rms* peculiar velocity averaged over all grid points agrees very well with

the value found by putting the simulation power spectrum into equation (11).

3.4 The Selection of Clusters

We define clusters in our simulations in the same way as White et al. (1993). High-density regions at $z = 0$ are located using a friends-of-friends group finder with a small linking length ($b=0.05$), and their barycentres are considered as candidate cluster centres. Any candidate centre for which the mass within $1.5 h^{-1}$ Mpc exceeds M_{min} is identified as a candidate cluster. The final cluster list is obtained by deleting the lower mass candidate in all pairs separated by less than $1.5 h^{-1}$ Mpc. In the following we will normally consider only clusters more massive than $M_{min} = 3.5 \times 10^{14} h^{-1} M_{\odot}$. The number of clusters found in each simulation is listed in Table 2. As already noted, the individual clusters in the different simulations of the matched set correspond closely. Despite the normalisation to cluster abundance it appears as though the SCDM model has significantly more clusters than the others. This is a reflection of its steeper power spectrum together with the value of M_{min} we have chosen. For $M_{min} = 5.5 \times 10^{14} h^{-1} M_{\odot}$ all the models have about 20 clusters.

We define the peculiar velocity of each cluster at $z = 0$ to be the mean peculiar velocity of all the particles within the $1.5 h^{-1}$ Mpc sphere. The peculiar velocity of the cluster at earlier times is taken to be the mean peculiar velocity of these particles. Consistent with this, we define the position of the cluster at each time to be the barycentre of this set of particles. At $z = 0$ this is very close to, but not identical with the cluster centre as defined above. We give the *rms* values of the initial (linear) and final ($z = 0$) peculiar velocities of the clusters in each of our models in Table 2. The initial values have been scaled up to the linear values predicted at $z = 0$. It is clear that these substantially underestimate the actual values, a result we discuss in more detail below. We note that the present-day properties of clusters in these simulations are considered in much more detail in Thomas et al. (1998).

4 COMPARISON OF THE PEAK MODEL WITH SIMULATIONS

4.1 The Cluster-Peak Connection

The extent to which dark haloes can be associated with peaks of the smoothed initial density field is somewhat controversial. Frenk et al. (1988) concluded that, for appropriate choices of filter scale and peak height, the correspondence is good, whereas Katz et al. (1993) claimed that “there are many groups of high mass that are not associated with any peak”. The result of correlating the peaks in the initial conditions of our simulations with the initial positions of our clusters is illustrated in Fig. 1. We consider a peak and a cluster to be associated if their separation is less than $4 h^{-1}$ Mpc (comoving). We find that the barycentres of 70% and 80% of the clusters with masses exceeding $3.5 \times 10^{14} h^{-1} M_{\odot}$ lie within of a peak with $\nu > 1.5$ for the low and high Ω models, respectively.

Fig. 1 shows that there is, as expected, a correlation

between the height of a peak and the mass of the corresponding cluster. In addition, combining the peak heights with the Δ values from Table 2, we see that the extrapolated *linear* overdensities of the peaks at redshift zero are similar but somewhat larger than the threshold value of 1.69 used in the standard Press-Schechter approach to analysing structure formation.

4.2 Linear Peculiar Velocities of Peaks and Clusters

Given the excellent correspondance between peaks of the smoothed linear density field and the initial positions of clusters, it is natural to compare the smoothed peculiar velocity at a peak with the mean initial peculiar velocity of its associated cluster. We show such a comparison in Fig. 2, again based on top-hat smoothing of both position and peculiar velocity fields using the characteristic radii listed in Table 2. All velocities are scaled up to the expected value at $z = 0$ according to linear theory. The correlation is clearly excellent in all cases, and is similar if gaussian rather than top-hat smoothing is used. The *rms* difference in peculiar velocity between a cluster and its associated peak is 16%, 16%, 23%, and 17% of the corresponding σ_p value listed in Table 2 for the OCDM, Λ CDM, SCDM and τ CDM simulations respectively. The somewhat larger percentage for the SCDM model is probably a consequence of the greater influence of small-scale power in this case.

4.3 The Growth of Cluster Peculiar Velocities

If cluster peculiar velocities grew according to linear theory the scaled initial velocities discussed in the last section and plotted in Fig. 2 would correspond to the actual velocities of the clusters at $z = 0$. In Fig. 3 we show scatter diagrams in which these two velocities are plotted against each other. It is evident that in fact the agreement is quite poor and that there is a systematic trend for the true cluster velocity to be larger than the extrapolated linear value. This is reflected in the substantial difference between the *rms* values of these two quantities listed in Table 2. It is presumably a consequence of nonlinear gravitational forces accelerating the clusters.

Some confirmation of this is provided by Fig. 4 where we plot the peculiar velocity in units of its initial value for five clusters from each of our cosmologies. At early times the peculiar velocities all grow as expected from linear theory (indicated in the figures by a dotted line) but at later times the behaviour is more erratic and most clusters finish with larger velocities than predicted.

Further evidence that late-time nonlinear effects are responsible for this discrepancy comes from Fig. 3. In this plot all clusters that have a neighbour within $10 h^{-1}$ Mpc are indicated with a diamond while more isolated clusters are indicated by a cross. It is evident that deviations from linear theory are substantially larger for the “supercluster” objects than for the rest. These objects also have systematically larger peculiar velocities at $z = 0$. Their *rms* peculiar velocity is around 20 to 30% larger than that of the sample as a whole.

For the τ CDM model, we have run a second realization

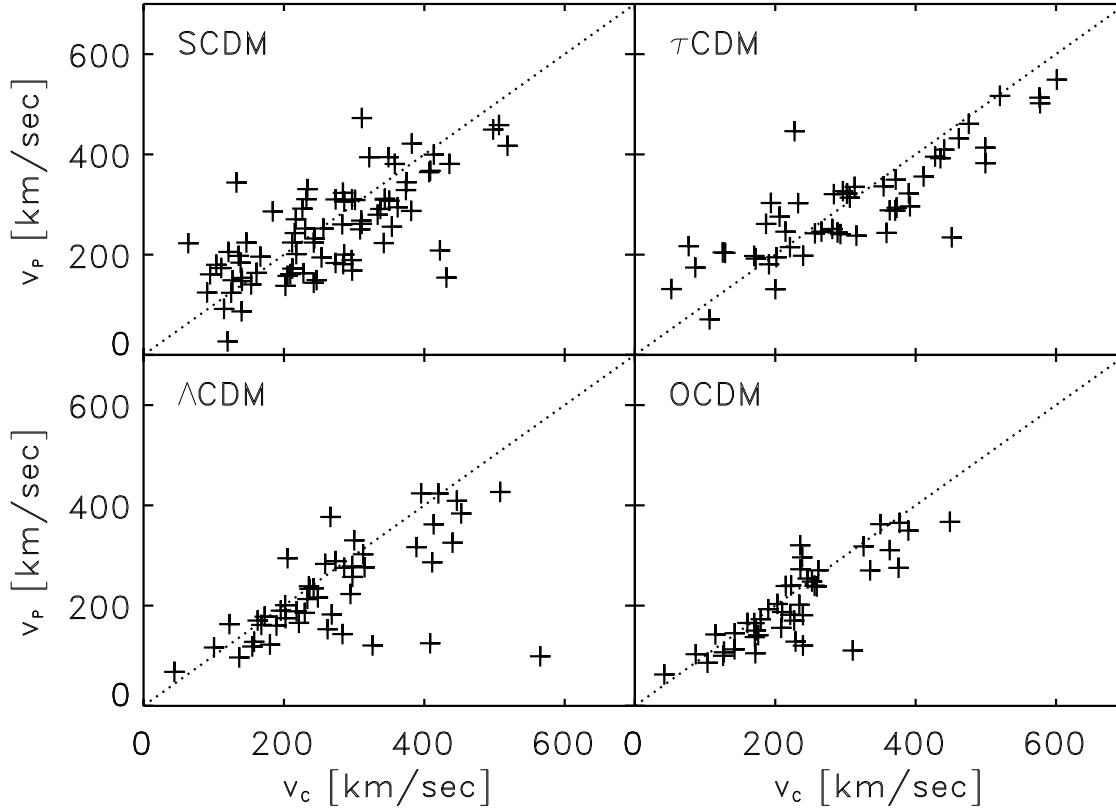


Figure 2. The initial peculiar velocities of clusters in each of our four cosmogonies are compared to the linear peculiar velocities of their associated peaks. The linear peculiar velocity field was smoothed with a top-hat in the same way as the density field in order to obtain the peak peculiar velocities.

of the power spectrum. We have extracted a cluster sample in the same fashion as described above. The *rms* peculiar velocity of the clusters at $z = 0$ is $\sigma_{z=0} = 511$ km/sec. The extrapolated *rms* linear peculiar velocity is $\sigma_{z=0} = 394$ km/sec. These numbers are very close to the values obtained for the first realization. Although two simulations are not a good statistical sample, we conclude that there is no realization dependence of the mis-match between the extrapolated linear and the actual peculiar velocities of galaxy clusters.

It might be thought that this anomalous acceleration of clusters at late times was a consequence of the relatively small radius, $1.5h^{-1}$ Mpc, which we use to define our clusters. Material could, perhaps be ejected asymmetrically from this region during the merging events by which clusters form. We have searched for such effects by redefining clusters to be all the material contained within a radius of 3 or $5h^{-1}$ Mpc and then repeating the analysis for the same set of objects as before. In most cases this turned out to make very little difference to either the initial or the final velocities measured, and it did nothing to reduce the discrepancy between them. The relevant nonlinear effects are acting on significantly larger scales. We repeated this procedure going as far out as $25h^{-1}$ Mpc from the cluster center. At a radius of $10h^{-1}$ Mpc, the difference between the *rms* peculiar velocity and the extrapolated *rms* linear peculiar velocity is only 10%. By a radius of $20h^{-1}$ Mpc, the numbers have finally converged.

The discrepancy between the *rms* peculiar velocity of clusters and their extrapolated *rms* linear peculiar velocity is

independent of any smoothing of the density field. With our choice of smoothing filter, the linear peculiar velocities of our clusters match those of their associated peaks as well as the *rms* value predicted by linear theory when the simulated realization of the power spectrum and the proper expression for the peculiar velocities (eq. 13) is used. Previous work (e.g. Borgani et al. 1997) has tried to match N-body data with linear theory by tuning the filter scale. Our results undermine the physical basis for such procedure.

5 CONCLUSIONS

We have investigated the peculiar velocities predicted for galaxy clusters by theories in the Cold Dark Matter family. A widely used hypothesis identifies rich clusters with high peaks of a smoothed version of the linear density fluctuation field. Their peculiar velocities are then obtained by extrapolating the similarly smoothed linear peculiar velocities at the positions of these peaks. We have tested this using a set of four large high-resolution N-body simulations. We identify galaxy clusters at $z = 0$ and then trace the particles they consist of back to earlier times. In the initial density field, the barycenters of 70% and 80% of the clusters with masses exceeding $3.5 \times 10^{14} h^{-1} M_{\odot}$ lie within $4h^{-1}$ Mpc (comoving) of a peak with $\nu > 1.5$ for the low and high Ω models, respectively. Furthermore, the mean linear peculiar velocity of the material which forms a cluster at $z = 0$ agrees well with the value at that peak.

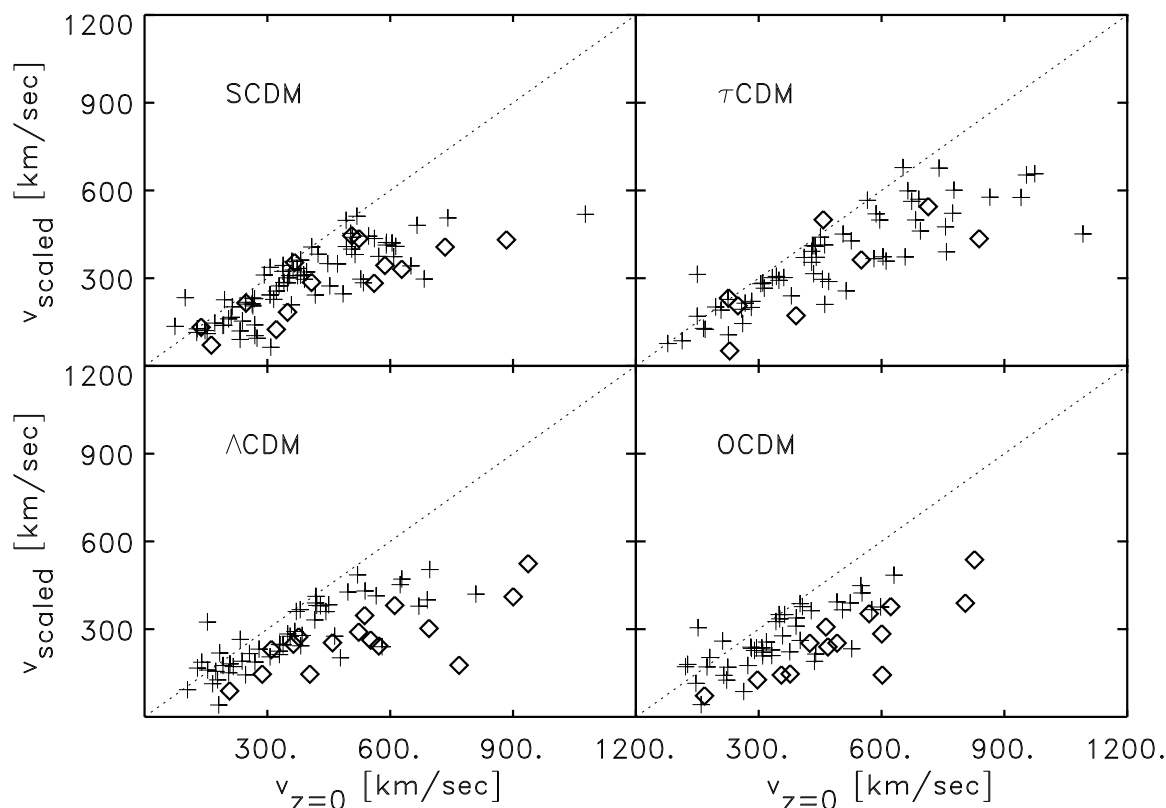


Figure 3. The initial peculiar velocities of clusters in each of our four cosmogonies, scaled up to $z = 0$ using linear theory, are compared to their actual peculiar velocities at $z = 0$. Diamonds denote clusters which have a neighbour within $10 h^{-1} \text{Mpc}$ while crosses denote more isolated clusters.

However, the late-time growth of peculiar velocities is systematically underestimated by linear theory. At the time clusters are identified, i.e. at $z = 0$, we find that the *rms* peculiar velocity is about 40% larger than predicted. Nonlinear effects are particularly important in superclusters; the *rms* values for clusters which are members of superclusters are about 20% to 30% larger than those for isolated clusters.

ACKNOWLEDGEMENTS

The simulations were carried out on the Cray T3D's and T3E's at the Computer Center of the Max-Planck-Gesellschaft in Garching and at the Edinburgh Parallel Computing Centre. Postprocessing was done on the IBM SP2 at the Computer Center of the Max-Planck-Gesellschaft in Garching. We thank George Efstathiou and John Peacock for valuable comments. JMC would like to thank Matthias Bartelmann, Antonaldo Diaferio, Adi Nusser, Ravi Sheth, and Mirt Gramann for numerous helpful and interesting discussions, and Volker Springel for providing his smoothing code.

This work was supported in part by the EU's TMR Network for Galaxy Formation. CSF acknowledges a PPARC Senior Research Fellowship.

REFERENCES

Bahcall N.A., Oh S.P., ApJ, 462L, 49B (1996)

- Bardeen J.M., Bond J.R., Kaiser N., Szalay A.S., ApJ, 304, 15 (1986) (BBKS)
 Bharadwaj S., Sethi S.K., ApJS, 114, 37B (1998)
 Bond, J.R., Efstathiou, G., ApJ, 285, L45 (1984)
 Borgani S., Da Costa L.N., Freudling W., Giovanelli R., Haynes M.P., Salzer J., Wegner G., ApJ, 482, L121 (1997)
 Carroll S.M., Press W.H., Turner E.L., ARAA, 30, 499 (1992)
 Couchman H.M.P., Thomas P.A., Pearce F.R., ApJ, 452, 797 (1995)
 Croft R.A.C., Efstathiou G., MNRAS, 268, L23 (1994)
 Efstathiou G., Davis M., Frenk C.S., White S.D.M., ApJS, 57, 241 (1985)
 Eisenstein D.J., astro-ph/9709054
 Eke V.R., Cole S., Frenk C.S., MNRAS, 282, 263 (1996)
 Frenk C.S., White S.D.M., Davis M., Efstathiou G., ApJ, 327, 507 (1988)
 Heath D.J., MNRAS, 176, 1 (1977)
 Jenkins A., Frenk C.S., Pearce F.R., Thomas P.A., Hutchings, Colberg J.M., White S.D.M., Couchman H.M.P., Peacock J.A., Efstathiou G.P., Nelson A.H., "The VIRGO Consortium: Simulations of Dark Matter and Galaxy Clustering", in Dark and Visible Matter in Galaxies and Cosmological Implications, eds Persic M., Salucci P., ASP Conference Series (1996)
 Jenkins A., Frenk C.S., Pearce F.R., Thomas P.A., Colberg J.M., White S.D.M., Couchman H.M.P., Peacock J.A., Efstathiou G.P., Nelson A.H. (The Virgo Consortium), ApJ, 499, in press (1998)
 Katz N., Quinn T., Gelb J.M., MNRAS, 265, 689 (1993) (KQG)
 Lahav O., Lilje P.B., Primack J.R., Rees M.J., MNRAS, 251, 128 (1991)
 MacFarland T., Pichlmaier J., Pearce F.R., Couchman H.M.P., A

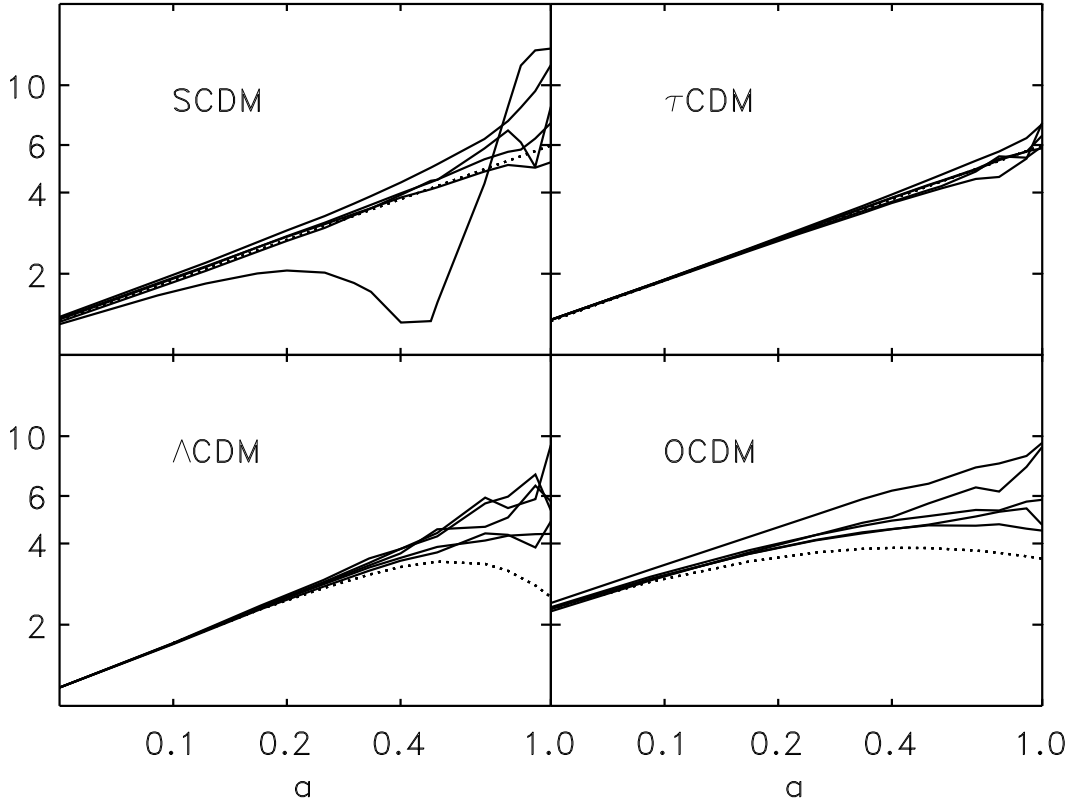


Figure 4. The evolution with expansion factor a of the ratio $|\vec{v}(a)|/|\vec{v}_0|$ for five clusters from each of our four cosmogonies (solid lines) is compared with the evolution predicted by linear theory (dotted line). In some of the cases, merging leads to abrupt changes in this ratio – the most impressive case can be seen for one of the SCDM clusters.

Parallel P3M Code for Very Large Scale Cosmological Simulations, presented at the European Cray-SGI MPP Workshop, Paris 1997, <http://www.rzg.mpg.de/~tmf/package/paper.html> (only Internet version available)

Monaco P., *Fund. Cosm. Phys.*, in press (1998)

Pearce F.R., Couchman H.M.P., Jenkins A.R., Thomas P.A., 'Hydra – Resolving a parallel nightmare', in *Dynamic Load Balancing on MPP systems*

Pearce, F.R., Couchman, H.M.P., "Hydra: A parallel adaptive grid code", submitted to *New Astronomy* (1997)

Peebles, P.J.E., *Principles of Physical Cosmology*, Princeton University Press 1993

Strauss, M.A., Willick, J.A., *Phys. Rep.*, 261, 271 (1995)

Sugiyama N., *ApJS*, 100, 281 (1995)

Thomas P.A., Colberg J.M., Couchman H.M.P., Efstathiou G., Frenk C.S., Jenkins A.R., Nelson A.H., Hutchings R.M., Peacock J.A., Pearce F.R., White S.D.M. (The Virgo Consortium) accepted by *MNRAS*, astro-ph/9707018

White M., Gelmini G., Silk J., *Phys. Rev. D*, 51, 2669 (1995)

White S.D.M., Efstathiou G., Frenk C.S., *MNRAS*, 262, 1023 (1993)